25th ABCM International Congress of Mechanical Engineering
October 20-25, 2019, Uberlândia, MG, Brazil

Stress State for Rotating Machine

Clodoaldo Borges Chagas
Marcos Vieira de Albuquerque
Robson Pederiva
University of Campinas – UNICAMP – School of Mechanical Engineering
cbchagas@fem.unicamp.br
marcosvieira@fem.unicamp.br
robson@fem.unicamp.br

Abstract. *The rotating machines are subjected to unbalanced rotors thus the shafts are loaded dynamically . The orbit of the geometric center of a cylindrical shaft differs as function of the angular velocity of this shaft. The stress state of a point on the surface of the shaft suffer alternation which is different from the behavior of a shaft with constant static load which is usually a sine wave. In Jeffcott rotors the unbalanced mass excites the system in forward direction changing the orbit of the shaft center from an elliptical shape to a line near to the first natural frequency. The present work models this phenomena to predict the stress state at some frequency operation using rotor dynamics theory applied for a rigid bearings model. The response for stress state is analyzed for under first critical angular velocity, subcritical velocity, between critical angular velocity for anisotropic system, and supercritical when the angular velocity is greater than the second critical angular velocity when the orbit of the shaft are practically circular. Close to the critical angular velocity, the shaft orbit tend to a line which cause an alternated stress state with average value different from zero. The response is not a perfect sine wave but is periodic and related to a complete loop of the shaft with frequency twice the system operation. This characteristic will be discussed.*

Keywords: *Rotor Dynamics, Rotating machine, Stress State*

1. INTRODUCTION

The rotor dynamic is an opened field for studies where some central subject are: dynamic behavior, identification and fail analysis, stability, mathematical models, bearing and foundation analysis (Sanches, 2015). The basics elements of a rotor are the disk, the shaft, the bearings, and the seals, Berthier *et al.* (1983), Lalanne *et al.* (1983) apud (Lalanne and Ferraris, 1990). Rotors of machine have a great deal of rotational energy and a small amount of vibration energy and the main purpose of the rotor dynamics is to keep this latter as small as possible, Kramer (1993). An intrinsic characteristic of the rotors is the unbalance, which causes vibrations. The unbalance occurs when the center of mass of the system rotor-shaft and its geometric center of spin are not coincident. The Fig. 1a) shows the most simple rotor which consist of massless shaft, at whose center is fixed to rigid circular disc and supported in rigid bearings. This model is called *Laval rotor* or *Jeffcott rotor.* In the Fig. 1a), C is the shaft geometric center, P is the center of mass of the disc, for unbalanced rotors the ε is the eccentricity. The axis between the bearings, O, is the center of rotation of the system. The unbalance causes a deflection of the shaft, as shown at left side of the Fig. 1a. For the case where the shaft is rigid and the bearings are softer the displacemnt is shown in the Fig. 1b.

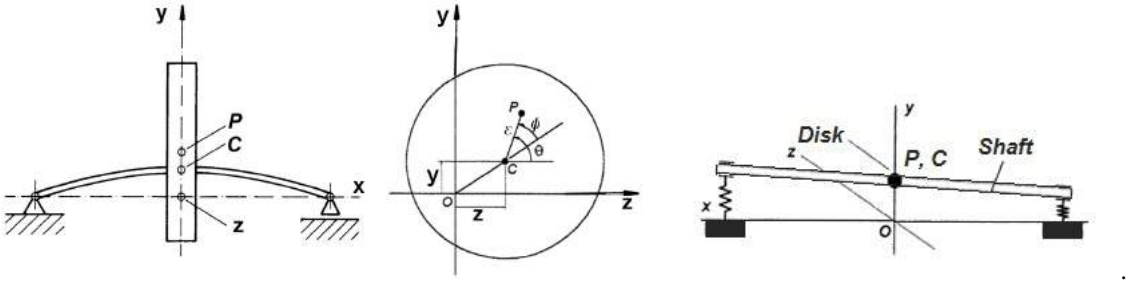

(a) (b)

Figure 1: Jeffcott Rotor – (a) Flexible Shaft *Source: Adapted from Kramer (1993)*; (b) Flexible Bearings and Rigid shaft *Source: Adapted from Souto (2000)*

The shaft bending is a function of the unbalanced mass and its position, the stiffness of the shaft and namely the

rotation ω. According to Pennacchi and et al. (2006) the identification of failures are one of the most important subject to be investigated. Thus, the bending of the shaft becomes important point of view because the shaft stress state may conduct the system to failure.

Case the shaft was much more stiff than the bearings, Fig. $1b$), the system could present only the rigid body modes. In the other wise, case the rotor stiff much less than the bearings the system will not present rigid body modes, Fig. $1a$), but only the precession modes, which could be roughly compared to the transverse vibration of a beam soft supported. Hence, the stiffness of the bearing and the shaft need to be considered in the model. In general, the shaft is commonly homogeneous but the bearings present anisotropic stiffness in both horizon and vertical direction. Thus, the combination of the shaft and bearings stiffness yields the general stiffness for each direction. For some cases, the characteristic of the rotor may become the gyroscopic effect neglected (Souto, 2000), as in the Jeffcoot Rotor where the disc is symmetric spaced from bearing with flexible shaft, for instance.

The vibration of a rotating machine can be described by the orbit of the geometric center of the rotor around the static equilibrium position (axis O of Fig. 1). Based on the precession motion, the gyroscopic effect causes the modes of vibration in forward direction, i. e. when the orbit motion of the center geometric C is at the same direction of rotor spin, or in backward direction, i. e. when the orbit motion of the geometric center C is in opposite to the rotor spin Gasch *et al.* (2006). There are more complex cases where some station of the shaft are in forward and others in backward precession direction, Genta (1999). In geneneral it is possible to assume that the rotors have three kinds of vibration: longitudinal, torsional and transversal. In most of cases this modes have little or, at least, no coupling between them and can be studied in separated way, Souto (2000). The precession motion loads the shaft in different ways. In the present work the stress state on the shaft surface will be discussed based on the parameter which may help to avoid jeopardizing conditions. Thus, It is important understand the dynamic of rotor first.

2. Jeffcott Rotor Model

2.1 Undamped Isotropic Model

For the scheme shown in the Fig. 1, the rigid disc is mounted at the middle of a flexible shaft. The disc is assumed to move only in its own plane. The position of the center of mass P relative to the unloaded position is in relation to y and z directions are y_1 and z_1, respectively. The angle between the line connecting the center of mass P and geometric center C makes an angle φ relative to the axis z. Thus, considering the non-damping free vibration of the Jeffcott Rotor for an isotropic system, the motion equations for the point P are written for the coordinate system showed in Fig. 1 as follow:

$$\begin{cases} m\ddot{y} + ky = 0 \\ m\ddot{z} + kz = 0 \end{cases} \tag{1}$$

The total stiffiness at any direction is k and the mass of the system is m. Supposing harmonic solution from $e^{j\lambda_n t}$, the solution of Eq. (1) is: $\lambda_n = \pm\sqrt{\frac{k}{m}}$, consequently, the general solution of Eq. (1) is:

$$\begin{cases} y = Y_1 e^{j\lambda_n t} + Y_2 e^{-j\lambda_n t} \\ z = Z_1 e^{j\lambda_n t} + Z_2 e^{-j\lambda_n t} \end{cases} \tag{2}$$

The point P motion, in the Fig. 1, is the combination of two harmonic motion of the same frequency which occurs in both direction y and z. These two motion create an elliptical trajectory of P around the axis through the bearings. This trajectory can be degenerated to circle or becomes a rectilinear one. The λ_n in the Eq. (2) is the natural frequency of harmonic oscillators that vibrate in two perpendicular axis y and z. The complex conjugate pair in the solution Eq. (2) present no physical sense, but it is necessary for the harmonic motion happens, according Euler relations. Another important feature is the rotating vector $e^{j\lambda_n t}$ where, only the real part has physical sense.

Writing the Jeffcott rotor motion in complex coordinates and defining the vector p as the position of the mass center P, $p = y + jz$, which rotate in the plane yz, Fig. 1, hence:
rewriting the equation of motion Eq. (1) in complex way: $m\ddot{p} + kp = 0$, and considering the harmonic solution: $p = Pe^{j\lambda_n t}$, the general solution of equation of motion is:

$$p = P_1 e^{j\lambda_n t} + P_2 e^{-j\lambda_n t} \tag{3}$$

with λ_n given by the homogeneous solution of Eq. (1).

Differently from the formulation in real coordinate system where λ_n only represent the natural frequency of harmonic oscillators, the use of complex coordinate allow to interpreted this term as the real precession velocity of the point P around the axis between bearings. The signal of λ_n points the direction of precession motion. According to the Eq. (3) the precession is a combination of circular motion of equal angular velocity which in opposite direction. The first, positive

term, occurs in the same direction of the shaft spin, called: *Forward.* The second, negative one, occurs in the opposite direction of the shaft spin, called: *Backward* (Lalanne and Ferraris, 1990). At the present work always the shaft spin will be considered positive.

The characteristics of the precession motion, shape and direction, are dependent from the relation between $|P_1|$ and $|P_2|$ (Gasch *et al.*, 2006), thus:

- If $|P_1| > |P_2|$ the P point describe a Forward precession with elliptical orbit;
- If $|P_1| < |P_2|$ the P point describe a Backward precession with elliptical orbit;
- If $|P_1| = |P_2|$ the P point describe a rectilinear motion;
- If $|P_1| \neq 0$ and $|P_2| = 0$ the P point describe a Forward precession with circular orbit;
- If $|P_1| = 0$ and $|P_2| \neq 0$ the P point describe a Backward precession with circular orbit;

The main advantages in using the complex coordinate to study rotor dynamics that is identify the direction of the precession orbit motion (Souto, 2000). The point P is not coincident at the geometric center of the disc C, Fig. 1, distant ε, this distance is the eccentricity and the O the axis between bearings, and calling $k/m = \omega_{cr}^2$, hence, the amplitude in the directions y and z are:

$$\begin{cases} Y = \varepsilon \dfrac{\omega^2}{\omega_{cr}^2 - \omega^2} \\ Z = \varepsilon \dfrac{\omega^2}{\omega_{cr}^2 - \omega^2} \end{cases} \tag{4}$$

For values of $\omega \to \infty$ the amplitude tend to zero, when the $\omega \to \omega_{cr}$ the amplitude of shaft bending tends to infinity, this is called critical angular velocity of the rotor (Genta, 1999).

It is common define two ranges of rotation, the first called *undercritical* when $\omega < \omega_{cr}$ and the second called *supercritical* when $\omega > \omega_{cr}$. In the region *supercritical* with $\omega \to \infty$ the amplitude of the precession orbit tends to be equal the eccentricity ε, according to eqs. (4) . This means, physically, that with the rising of the angular velocity the rotor tends to turn around the mass center P and not around the geometry center C. This phenomenon is known as *selfcentering* (Souto, 2000).

2.2 Undamped Anisotropic Model

For an axissimetric rotor supported by bearings with different stiffness in the y and z directions, the polar diagram of stiffness is an ellipse known as elasticity ellipse (Genta, 1999).

Different from isotropic model where the motion equation in both direction are equals, in the anisotropic model they are not coincident. When solved the homogeneous associated system yields two different natural frequencies, $\lambda_y = \pm\sqrt{\dfrac{k_y}{m}}$ and $\lambda_z = \pm\sqrt{\dfrac{k_z}{m}}$, in the y and z direction, respectively.

The modal parameters are independent from rotation, hence there are two critical angular velocity which could be coincident to the rotor velocity. For the free response of the anisotropic system the following parameter should be introduced:

$$\begin{cases} k_m = \dfrac{(k_y + k_z)}{2} \\ k_d = \dfrac{(k_y - k_z)}{2} \end{cases} \tag{5}$$

Rewriting the motion equation in complex coordinate and adding the parameters from Eq. (5), the homogeneous problem is given by:

$$m\ddot{p} + k_m p + k_d \overline{p} = 0 \tag{6}$$

where $\overline{p}$ the complex conjugate of p, for proposed solution of the same kind of Eq. (3). Substituting into homogeneous motion equation and rearranging the terms:

$$\left(\lambda^2 \begin{bmatrix} m & 0 \\ 0 & m \end{bmatrix} + \begin{bmatrix} k_m & k_d \\ k_d & k_m \end{bmatrix}\right) \begin{Bmatrix} P_1 \\ \overline{P_2} \end{Bmatrix} = \begin{Bmatrix} 0 \\ 0 \end{Bmatrix} \tag{7}$$

When solved the Eq. (7) the same natural frequencies are found, substituting these values in the proposed solution and rearranging the terms it is possible to reach the solution in general form (Souto, 2000):

$$p = P_{F1}e^{j\lambda_n t} + P_{F2}e^{-j\lambda_n t} + P_{B1}e^{j\lambda_n t} + P_{B2}e^{-j\lambda_n t} \tag{8}$$

Substituting the λ_y into the eq. (7) reaches in relation $P_1/\overline{P_2} = -1$, and in analog way, substituting the λ_z into (7) the relation got is $P_1/\overline{P_2} = 1$. It is possible to note that for this case $P_{B1}/\overline{P_{B2}} = -1$ and $P_{F1}/\overline{P_{F2}} = 1$. Based on isotropic case, the precession motion of the rotor will be rectilinear when the angular velocity of the rotor coincide with any of the natural frequencies, due to $|P_{B1}| = |\overline{P_{B2}}|$ for the first backward mode and $|P_{F1}| = |\overline{P_{F2}}|$ in the second forward mode.

The precession components forward, P_1, and backward, P_2, are:

$$\begin{aligned} P_1 &= \frac{\left(k_m - m\omega^2\right)\left(m\varepsilon\omega^2\right)}{\left(k_y - m\omega^2\right)\left(k_z - m\omega^2\right)} \\ P_2 &= \frac{-k_d m\varepsilon\omega^2}{\left(k_y - m\omega^2\right)\left(k_z - m\omega^2\right)} \end{aligned} \tag{9}$$

The unbalance response will be:

$$p = \frac{\left(m\varepsilon\omega^2\right)}{\left(k_y - m\omega^2\right)\left(k_z - m\omega^2\right)}\left[\left(k_m - m\omega^2\right)e^{j\omega_n t} - k_d e^{-j\omega_n t}\right] \tag{10}$$

When the Eq. (9) and (10) are analyzed it is possible to conclude some important information about the anisotropic rotor under synchronous unbalancing excitation force:

- When the stiffness in y and z are equals, the P_1 value will be the same as the isotropic, and P_2 becomes null;
- The response amplitude tends to infinity always that the rotation comes near to either $\sqrt{k_y/m}$ or $\sqrt{k_z/m}$, this means that there are two critical velocities, which become the denominator of Eq. (10) null;
- The backward components will not be null for anisotropic bearings $k_d \neq 0$;
- When the angular velocity of the rotor $\omega = \sqrt{k_m/m}$ the contribution of forward mode under unbalancing will be null, in this case the precession motion presents only the backward precession mode with circular orbit;
- Case $k_d \approx 0$, this means that rotor system is almost isotropic, or little anisotropic, with almost similar stiffness in both direction, y and z , the backward component will be very small, $|P_2| \to 0$.

The direction of the precession motion of geometric center C, Fig. 1, it is defined by the amplitudes of the forward and backward precession coefficients, P_1 and P_2, respectively. The present work shows the results for a rotor system with $m = 1.0\ kg$, $\varepsilon = 1 \cdot 10^{-3}\ m$, $k_y = 1 \cdot 10^5\ N/m$ and $k_z = 2 \cdot 10^4\ N/m$. When $|P_1| < |P_2|$, this means, $|P_1|/|P_2| < 1$, the precession of the rotor will be backward, this phenomenon happens between both critical angular velocity λ_z and λ_y. When the angular velocity of the rotor closes to any one of both critical velocity the precession orbit will become rectilinear. The precession orbit out of the critical velocities range always be elliptical with forward precession. The ratio $|P_1|/|P_2|$ rises with the rotation, in the super critical range, leaving clear the dominance of forward coefficient, $|P_1|$, this characteristic tends to keep the elliptical precession orbit degenerated to a circle, the selfcentering.

The identification of the shape and direction of the precession motion are of great value because these characteristic present important information about the stress state of the shaft (Souto, 2000).

2.3 Damped Anisotropic Model

The rotor systems used to be damped (Gasch *et al.*, 2006), considering the viscous damping coefficient for the direction y and z, c_y and c_z, respectively, and introducing the parameters:

$$\begin{cases} c_m = \dfrac{c_y + c_z}{2} \\ c_d = \dfrac{c_y - c_z}{2} \end{cases} \tag{11}$$

The motion equation for the Jeffcott damped system in complex coordinate with excitation by unbalance is:

$$m\ddot{p} + c_m\dot{p} + c_d\dot{\overline{p}} + k_m p + k_d\overline{p} = m\varepsilon\omega^2 e^{j\omega t} \tag{12}$$

The precession amplitude coefficient solution for forward, P_1, and backward, P_2, are:

$$\begin{cases} P_1 = \dfrac{\left(k_m + j\omega c_m - m\omega^2\right)\left(m\varepsilon\omega^2\right)}{\left(k_y + jc_y - m\omega^2\right)\left(k_z + j\omega c_z - m\omega^2\right)} \\ P_2 = \dfrac{-\left(j\omega c_d + k_d\right)\left(m\varepsilon\omega^2\right)}{\left(k_y + jc_y - m\omega^2\right)\left(k_z + j\omega c_z - m\omega^2\right)} \end{cases} \tag{13}$$

Case the damping coefficients were null the Eq. (13) becomes Eq. (9).

The Fig. 2a shows the ratio between the forward and backward amplitudes, $|P_1|/|P_2|$ as function of angular velocity, considering c_y, equal to 0, 25, 50, 100, 250 and 500 Ns/m and in the z direction, c_z, will be a proportion $\alpha = 0.2$ of c_y, for the same condition related in the section 2.2

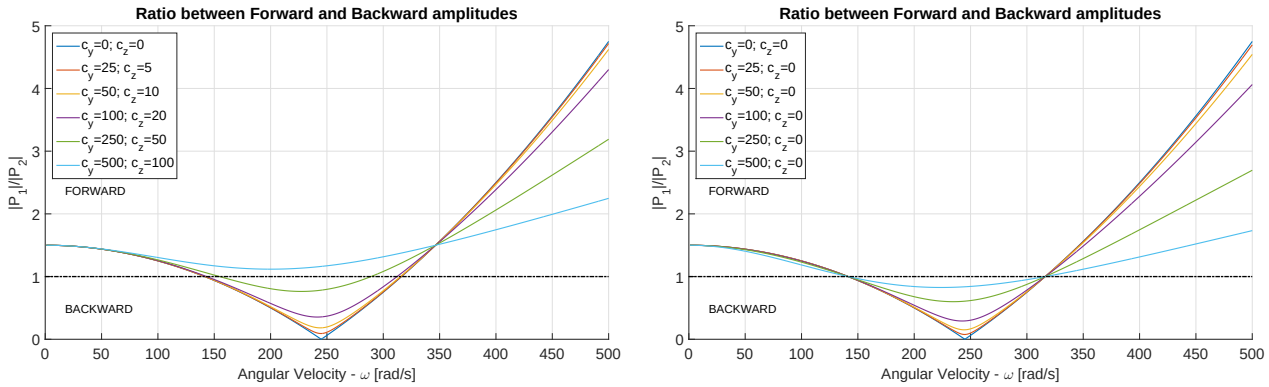

(a) $c_z = \alpha c_y$ (b) $c_y \neq 0$; $c_z = 0$

Figure 2: Relation between forward and backward amplitudes in function of the rotation for anisotropic damped system

Observing the Fig. 2a, when the damping factor rises the range when the backward precession occurs, i. e. when the orbit becomes rectilinear, $|P_1|/|P_2| = 1$, becomes smaller, and the orbit will not be perfectly circular, as for non damped case, because always there are a forward coefficient $|P_1| \neq 0$. For the special case when $c_y = 500\ Ns/m$ and $c_z = 100\ Ns/m$ are not found values of the ratio $|P_1|/|P_2| < 1$, that is, the backward precession will not be observed at any rotation range. Another important to be noted is the self-centering which tends to happen at higher angular velocity with the increase of damping coefficient.

For unidirectional damping coefficient, for instance $c_y \neq 0$ and $c_z = 0$, does not occurs the narrowing of the backward precession range. The analyzed cases, shown in the Fig. 2b, all curves intercepted at abscissas λ_y and λ_z with ordinate $|P_1|/|P_2| = 1$. However, with the increase of the damping coefficient the ratio $|P_1|/|P_2| \approx 1$ in super critical velocity range, which tends to become the forward precession orbit to become rectilinear in the direction of the null coefficient. The physical interpretation is due to the fact that in one of the directions there is resistance to motion and in another there are no resistance. This observation is important because the backward range jeopardize the shaft more than the forward region and will proved in the present work. The rotors system which may added some viscous damping, such as the use of pads, in only one direction will not narrow the backward range.

The Fig. 3 shows the orbit of geometric center of an anisotropic Jeffcott rotor under unbalance with $m = 1.0\ kg$, $\varepsilon = 1 \cdot 10^{-3}\ m$, $k_y = 1 \cdot 10^5\ N/m$, $k_z = 2 \cdot 10^4\ N/m$, $c_y = 25\ Ns/m$ and $c_z = 5\ Ns/m$ as function of the angular velocity. These kind of figure is called *orbital tube* (Genta, 1999).

Analyzing the Fig. 3 with help from figures 4a and 4b it is possible to note that the amplitude of the orbit increase near to the first angular velocity $\lambda_z = 141.4\ rad/s$. Following the second critical angular velocity the orbit decrease and tends to stabilized with super critical velocities with orbit equal to the eccentricity ε. The figures 4a and 4b show the orbital tube in the planes xy and xz, respectively. These kind of figures are called orbital view.

The main axis of the precession ellipse change the direction at each shaft angular velocity. The orbital view at the Fig. 4 show this behavior. At the first critical velocity the orbital becomes linear with direction z axis, at $\lambda_z = 141.4\ rad/s$. Close to the second critical velocity, $\lambda_y = 316.2\ rad/s$, the main axis of the precession ellipse is in the direction of y. For some rotor system where there are the possibility of the use of instrumentation able to measure the stress state on the shaft surface such as strain gauges, the values measured have great chance to are not the main values, or values less than ones who will promote the system failure. The gauges, for example, could measure only the main stress state at some specific velocity and for another the values may be not concerning.

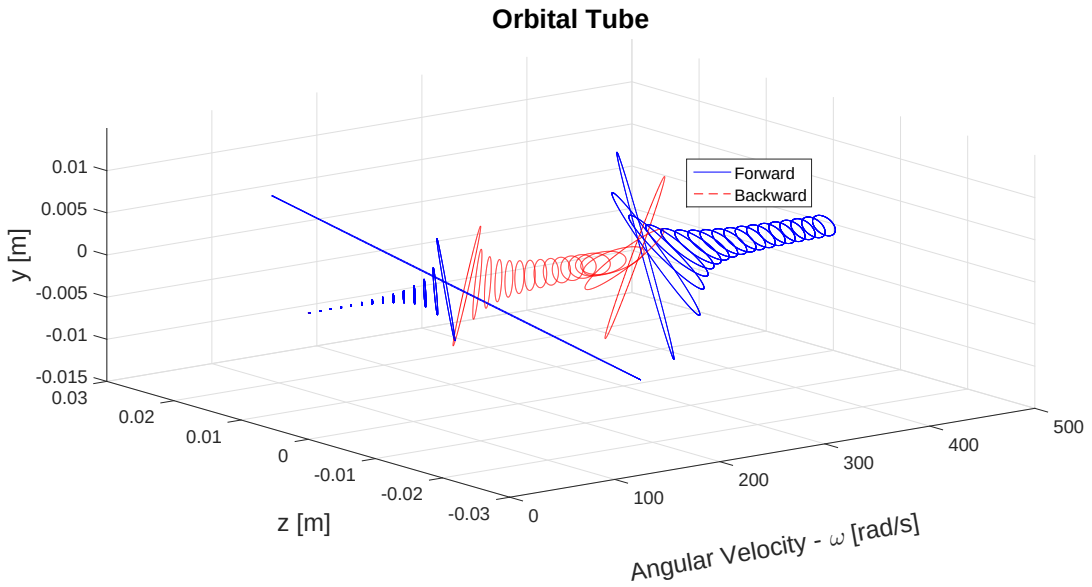

Figure 3: Anisotropic Jeffcott rotor system response under unbalancing – *Orbital Tube* for $m = 1.0\ kg$, $\varepsilon = 1 \cdot 10^{-3}\ m$, $k_y = 1 \cdot 10^5\ N/m$, $k_z = 2 \cdot 10^4\ N/m$, $c_y = 25\ Ns/m$ and $c_z = 5\ Ns/m$.

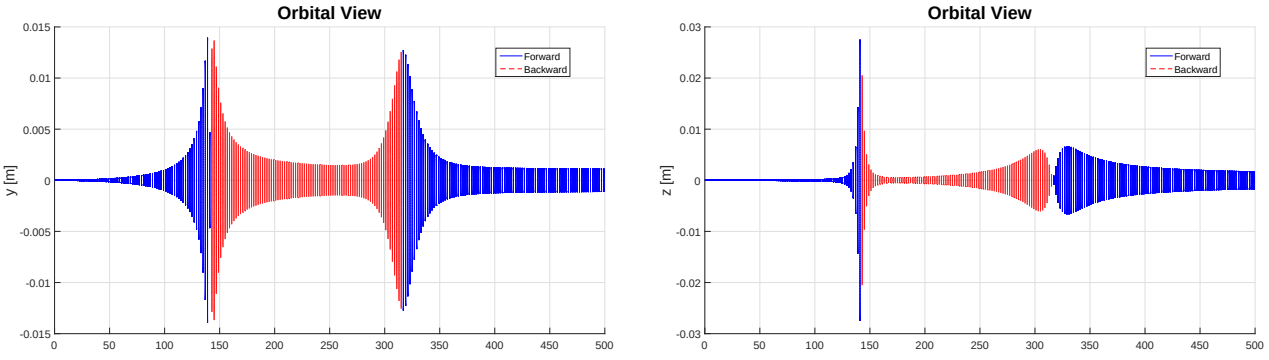

(a) Plane xy (b) Plane yz

Figure 4: Anisotropic Jeffcott rotor system response under unbalancing – *Orbital view* for $m = 1.0\ kg$, $\varepsilon = 1 \cdot 10^{-3}\ m$, $k_y = 1 \cdot 10^5\ N/m$, $k_z = 2 \cdot 10^4\ N/m$, $c_y = 25\ Ns/m$ and $c_z = 5\ Ns/m$.

2.4 Behavior of shaft surface at Forward and Backward precession

The Fig. 5 shows the succession of events for a Jeffcott rotor with $m = 1.0\ kg$, $\varepsilon = 1 \cdot 10^{-3}$, $k_y = 1 \cdot 10^5\ N/m$, $k_z = 2 \cdot 10^4\ N/m$, $c_y = 50\ Ns/m$, $c_z = 10\ Ns/m$ at angular velocity $\omega = 100\ rad/s$ and forward precession. In the Fig. 5 the points O, C and P are the axis between bearings, the geometric center of rotor, and the mass center, respectively. The red circle represent a circular shaft, the blue ellipse is the orbit of the geometrical center runs. The shaft is on clockwise, consequently, due to the motion is on forward the motion of the geometric center C is also in clockwise. The M point represent the more remote fiber on the shaft surface when the geometric center C is farther from the axis O, between bearings. The M point will suffer the maximum deformation on the shaft surface. The N point is on the neutral deformation plane at the beginning of the motion, $t = 0$.

The Fig. 7a shows the relative distance of the points M and N, on the surface of the shaft in relation of the instantaneous neutral plane. This relative distance of the analyzed points are divided by the radius of the shaft to become a dimensionless measure.

The Fig. 6 shows the succession of events for the same Jeffcott rotor presented in the Fig. 5, but at $\omega = 230\ rad/s$, this means that the rotor is under backward precession motion, hence, the shaft is on clockwise and the motion on the elliptical orbit of the geometric center C is on counterclockwise. The behavior of the point M and N for one complete turn of the shaft is presented in the Fig. 7b.

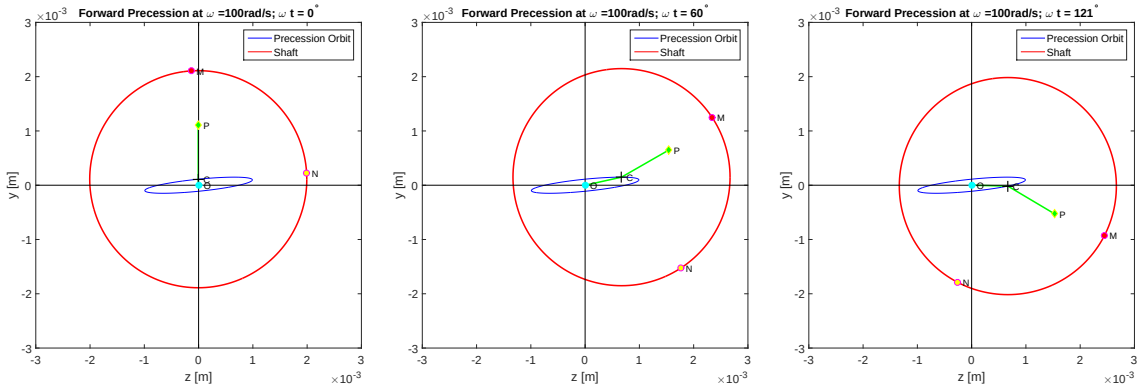

(a) 0° (b) 60° (c) 121°

Figure 5: Succession of events at Forward direction $\omega = 100\ rad/s$ for $m = 1.0\ kg$, $\varepsilon = 1 \cdot 10^{-3}\ m$, $k_y = 1 \cdot 10^5\ N/m$, $k_z = 2 \cdot 10^4\ N/m$, $c_y = 25\ Ns/m$ and $c_z = 5\ Ns/m$.

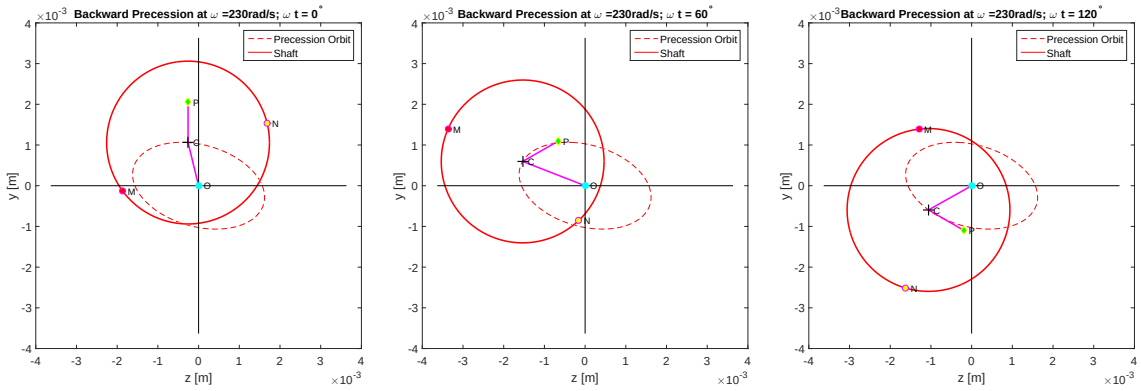

(a) 0° (b) 60° (c) 120°

Figure 6: Succession of events at Bacward direction $\omega = 230\ rad/s$ for $m = 1.0\ kg$, $\varepsilon = 1 \cdot 10^{-3}\ m$, $k_y = 1 \cdot 10^5\ N/m$, $k_z = 2 \cdot 10^4\ N/m$, $c_y = 25\ Ns/m$ and $c_z = 5\ Ns/m$.

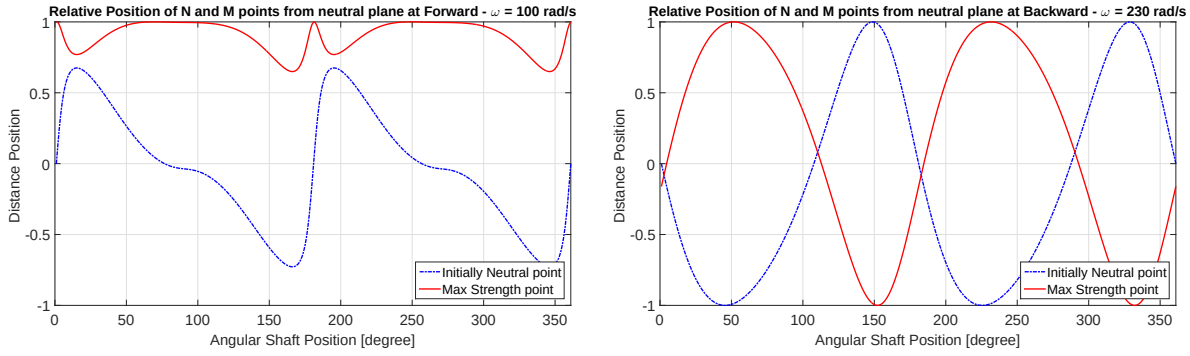

(a) Forward $\omega = 100\ rad/s$ (b) Backward $\omega = 230\ rad/s$

Figure 7: Distance relative of the point M and N on shaft surface.

2.5 Deflection of the Shaft

In the present work the displacement of the geometric center C, is attributed only to the shaft, according Fig. $1a$), although, in the real case there is some displacement of the bearings such as shown in the Fig. $1b$) added to the shaft deflection. This consideration is conservative regarding to the life in fatigue of the shaft. The shaft is considered a prismatic beam and the formulation used to determine the neutral axis of the shaft is according this kind of beam.

For the Jeffcott rotor the maximum deflection occurs at the position of the disc who is centered at $x = L/2$.

$$r(P) = \frac{PL^3}{48EI} \tag{14}$$

The Eq. (14) is linear and correlates the load P to the displacement of the neutral axis into shaft to the bearing axis for a transverse load. The deflection of the shaft may be interpreted as the distance between the point C to the axis O for any position of the orbit of the geometrical center of Jeffcott rotor. The maximum bending moment at the center of the beam $x = L/2$ is calculated as:

$$M_{max} = \frac{PL}{2} \tag{15}$$

the maximum stress state at the fiber most distant from the neutral axis is determined by Beer *et al.* (2011):

$$S_{max} = \frac{M_{max}c}{I} \tag{16}$$

Considering a Jeffcott rotor of structure steel shaft ($ASTM - A913\ Grade\ 450$) with Young Modulus $E = 200\ GPa$, yield strength $\sigma_e = 450\ MPa$ (Beer *et al.*, 2011), length $L = 0.3\ m$ and constant cross section with diameter $d = 10 \cdot 10^{-3}\ m$. Hence the transverse moment of inertia $I = \frac{\pi R^4}{4} = 4.91 \cdot 10^{-10}\ m^4$.

2.6 Stress State

How the shaft has been considered as a beam, the line whose cross through the geometrical center C can be assumed as its neutral stress state axis. Then, using a referential linked to the shaft, the differential elements on the shaft surface, i.e. the points M and N, from Fig. 5 and 6, have the stress state studied in this section.

The unbalance allied to the anisotropic bearings promotes the elliptical orbits of the geometrical center of the rotor, hence using the displacement of the geometric center presented in the section 2.3 it is possible determine the transverse load whose would cause those displacement, according to section 2.5 to determine the bend moment, Eq. (15), and the stress state on the shaft surface, Eq. (16).

During the revolution of the shaft and the orbit assumed by the disc center, as disposed in the figures 5 and 6, the stress state on the shaft surface near to the disc is not constant. Figures 8a and 8b show the stress state for the points M and N in forward and backward precession at 100 rad/s and 230 rad/s, respectively.

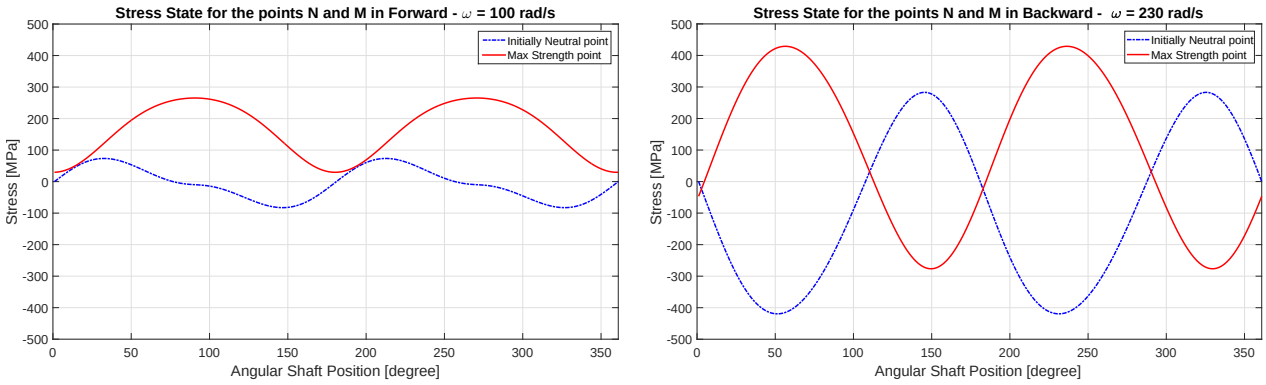

(a) Forward precession at 100 rad/s (b) Backward precession at 230 rad/s

Figure 8: Stress State for the points M and N at Forward and Backward precession.

Observing the forward precession, Fig. 8a, the point N, who initiates the motion on the neutral plane of stress, it oscillates around the null stress. In the other wise, the point M, who is under the maximum stress at $t = 0$, it always reaches positive stress state, due to the bending is always at the same direction for a referential linked to the shaft. The frequency of loading is two times the spin frequency. Analyzing the stress state at backward precession, Fig. 8b, both studied points, M and N have oscillation of the stress state between positive and negative, this means that the shaft change the stress state from compression to stretch with frequency two times the spin frequency. Although the loading frequency are two times the spin frequency for both case (forward and backward precession), in the backward precession the peak to peak values are larger than the another one. Therefore, these elements reach stretch stress state cycling due to the elliptical orbit. In contrast, if an element which is pointed to the center of the orbit always reaches compression stress state. Case the precession motion were perfectly circular the stress state would be constant at forward precession and the stress state

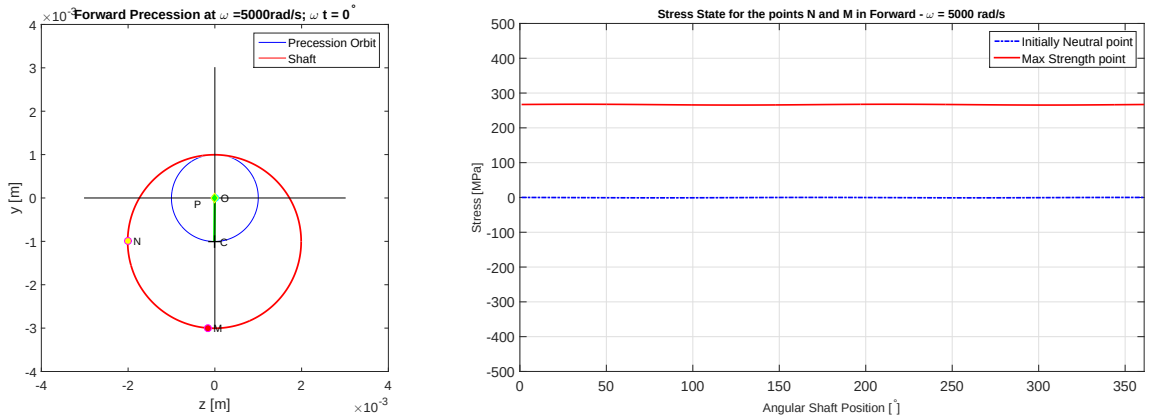

(a) (b)

Figure 9: Circular orbit, (a) due to self-centering at forward precession at $5000\ rad/s$, (b) steady state for the stress state of the points M and N for circular orbit.

would be sinusoidal at backward precession, since the own weight is neglected. However, the orbit is elliptical and it promotes the oscillation of the stress state. The motion at high spin, for instance at $5000\ rad/s$, for the Jeffcott rotor discussed in this paper, experimented the self-centering phenomena and the motion becomes around the center of mass P who tend to belong to the axis of the bearings O hence the orbit is circular. The Fig. 9a and 9b show the orbit with self-centering and the stress state for the points M and N, respectively at $5000\ rad/s$.

3. Conclusion

The present work discussed about the orbit for different conditions of damping and rotation using complex coordinate system to interpret the physical phenomena. The methodology consist to identify the eigens frequencies for the orthogonal direction of the bearings.

Some considerations can be inferred about the stress state in shaft from the dynamic behavior analysis in different range of angular velocity of the rotor, they are:

- Case the precession motion was in forward direction with circular orbit an observer fixed to the shaft does not identify changes in the stress state of the shaft, Fig. 9;
- Case the precession motion was in forward direction with elliptical orbit an observer fixed to the shaft will only identify changes in the magnitude of the stress state, Fig. 8a;
- Case the precession motion was in backward direction an observer fixed to the shaft will identify changes in the magnitude (amplitude of the stress) and in modulus (sense of stress – stretch or compression) of the stress state of the shaft, this means stretch and compression, Fig. 8b. This condition promotes the interchange of the stress state which allows the premature failures by fatigue;
- The use of viscous damping at both direction y and z narrows the backward range, this consideration can be beneficial for rotor system that operate between both critical velocity, although for super critical machines the damping postpone the selfcentering, Fig. 2a. Rotor system which needs to reach supercritical velocities may be helped to pass for the backward region when the damping coefficient are significant;
- The use of viscous damping at only one direction do not show advantages to reduce backward range, where the stress state cycling is more damage to the shaft, Fig. 2b;

In the present work the own weight was not considered, for the cases were for horizontal shaft the mass under gravity could bend the shaft. Consequently the shaft deflection due to field force may be greater than the precession ellipse, when this condition happen the forward motion will present alternation in module of stress state for critical elements on the shaft surface.

The techniques presented here allow the rotate machinery designer to predicted the precession orbit for a Jeffcott rotor using some parameters such as shaft length, diameter, material properties, bearings stiffness, disc mass and its excentricit. Consequently, the deflection of the shaft due to the unbalance force loads the system and the stress state on the shaft surface can be determined by the techniques exposed. The use of the appropriated formulation shown the large amplitude for the stress state on the shaft surface when the precession is at backward sense. The designer may use the

methodology proposed to minimize the range of backward precession. The backward has been shown more harmful to the shaft. Another important feature predicted by the proposed methodology concerns to the constant stress state on the shaft surface at high spin velocity, when the self centering phenomena occurs. For forward precession with spin bellow the first critical angular velocity the stress state are cyclic but the amplitude is lower than that ones found in backward precession. The presented methodology may help the designer to avoid the range of the angular velocity of the rotor where the conditions will jeopardize the shaft in fatigue life.

4. ACKNOWLEDGEMENTS

The authors would like to thank CAPES and grant # 2015/20363-6 from the São Paulo Research Foundation (FAPESP) for the financial support to this research. for the financial support of this research.

5. REFERENCES

Beer, F., Jr. Johnston, E., DeWolf, J. and Mazurek, D., 2011. *Mechanics of Materials*. McGraw-Hill Education. ISBN 9780073380285.

Berthier, P., Ferraris, G. and Lalanne, M., 1983. "Prediction of critical speeds, unbalance and nonsynchronous forced response of rotors". *53th Shock and Vibration Bulleting*.

Gasch, R., Nordmann, R. and Pfützner, H., 2006. *Rotordynamik*, Vol. 2. Springer. ISBN 3-540-41240-9.

Genta, G., 1999. *Vibrations of structures and machines: practical aspects*. New York: Springer Verlag.

Kramer, E., 1993. *Dinanic of Rotors and Foundations*. Springer-Verlag, Berlim Heidelberg.

Lalanne, M., Berthier, P. and Der Hagopian, J., 1983. *Mechanical Vibration for Engineers*. John Wiley.

Lalanne, M. and Ferraris, G., 1990. *Rotordynamics Prediction in Engineering*. 1st edition.

Pennacchi, P. and et al., 2006. "Use of modal representation for the supporting structure in model-based fault identification of large rotating machinery: part 1 - theoretical remarks". *Mechanical Systems and Signal Processing*, Vol. 20, No. 3, pp. 662–681.

Sanches, F.D., 2015. *Identificação simultânea de desbalanceamento e empeno de eixo em rotores através de analise de correlações*. Ph.D. thesis, Campinas - SP.

Souto, C.d., 2000. *Estudo do comportamento dinâmico de máquinas rotativas através da analise modal complexa*. Master's thesis, Unicamp - SP. URL `http://repositorio.unicamp.br/jspui/handle/REPOSIP/263791`.